ACS SyntheticBiology

pubs.acs.org/synthbio Research Article

Metabolic Engineering of *Saccharomyces cerevisiae* for High-Level Production of Chlorogenic Acid from Glucose

Feng Xiao, Jiazhang Lian, Shuai Tu, Linlin Xie, Jun Li, Fuming Zhang, Robert J. Linhardt, Haichan Huang, and Weihong Zhong*

Cite This: *ACS Synth. Biol.* 2022, 11, 800–811 Read Online

ACCESS | Metrics & More | Article Recommendations | Supporting Information

ABSTRACT: Chlorogenic acid (CGA), a major dietary phenolic compound, has been increasingly used in the food and pharmaceutical industries because of its ready availability and extensive biological and pharmacological activities. Traditionally, extraction from plants has been the main approach for the commercial production of CGA. This study reports the first efficient microbial production of CGA by engineering the yeast, *Saccharomyces cerevisiae*, on a simple mineral medium. First, an optimized *de novo* biosynthetic pathway for CGA was reconstructed in *S. cerevisiae* from glucose with a CGA titer of 36.6 ± 2.4 mg/L. Then, a multimodule engineering strategy was employed to improve CGA production: (1) unlocking the shikimate pathway and optimizing carbon distribution; (2) optimizing the L-Phe branch and pathway balancing; and (3) increasing the copy number of CGA pathway genes. The combination of these interventions resulted in an about 6.4-fold improvement of CGA titer up to 234.8 ± 11.1 mg/L in shake flask cultures. CGA titers of 806.8 ± 1.7 mg/L were achieved in a 1 L fed-batch fermenter. This study opens a route to effectively produce CGA from glucose in *S. cerevisiae* and establishes a platform for the biosynthesis of CGA-derived value-added metabolites.

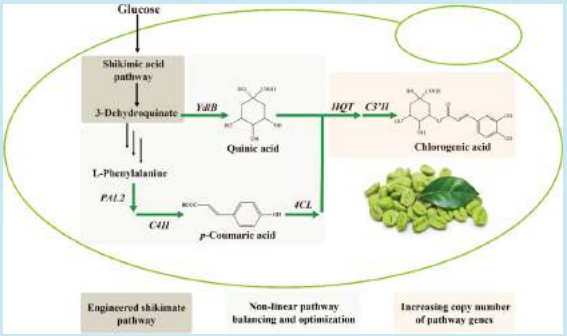

KEYWORDS: *chlorogenic acid, Saccharomyces cerevisiae, metabolic engineering, de novo biosynthesis, pathway balancing, nonlinear biosynthetic pathway*

Due to health concerns with traditional chemical preservatives in the food industry, there has been growing attention toward natural and herbal substitutes. Phenolic acids are such a family of compounds due to their anti-inflammatory and antioxidant properties. Chlorogenic acid (CGA, 3-*O*-caffeoylquinic acid), one of the most important dietary phenolic acid compounds, is commonly found in foods and herbs with a relatively high abundance in green coffee beans. Pharmacological research has demonstrated that CGA exhibits various health-promoting properties including antioxidant, anti-inflammatory, antimicrobial, antiviral, antilipidemic, antiobesity, antidiabetic, antihypertensive, antitumor, hepatoprotective, and neuroprotective activities.[1−5] Therefore, CGA is generally considered as an ideal nutraceutical and food additive with great potential in food and pharmaceutical industries.[3,5,6] Despite its established market and expanded applications, current phytoextraction-based production approaches are energy-intensive and environmentally unfriendly. Alternatively, the microbial production of CGA using synthetic biology and metabolic engineering can provide a sustainable and cost-effective way to meet the growing market and reduce the cost of CGA.

Biosynthesis of CGA in plants takes place in the shikimic acid (SA) pathway and involves a diverging−converging route mediated by hydroxycinnamoyl-CoA quinate transferase (HQT), which uses caffeoyl-CoA or *p*-coumaroyl-CoA as the donor and quinic acid (QA) as the acceptor (Figure S1A).[7] QA, an intermediate of the SA pathway, is synthesized from 3-dehydroquinate (DHQ) by QA dehydrogenase. The formation of caffeoyl-CoA or *p*-coumaroyl-CoA is catalyzed by 4-coumaroyl-CoA ligase (4CL) with caffeic acid (CA) or *p*-coumaric acid (PA) as the substrate. The synthesis of PA is derived from L-phenylalanine catalyzed by plant L-phenylalanine ammonia lyase (PAL), cinnamate-4-hydroxylase (C4H), and its associated cytochrome P450 reductase (CPR) or from L-tyrosine through microbial L-tyrosine ammonia lyase (TAL) (Figure 1). There are two possible routes proposed for microbial CGA production. In route 1

Received: September 30, 2021
Published: February 2, 2022

https://doi.org/10.1021/acssynbio.1c00487
ACS Synth. Biol. 2022, 11, 800–811

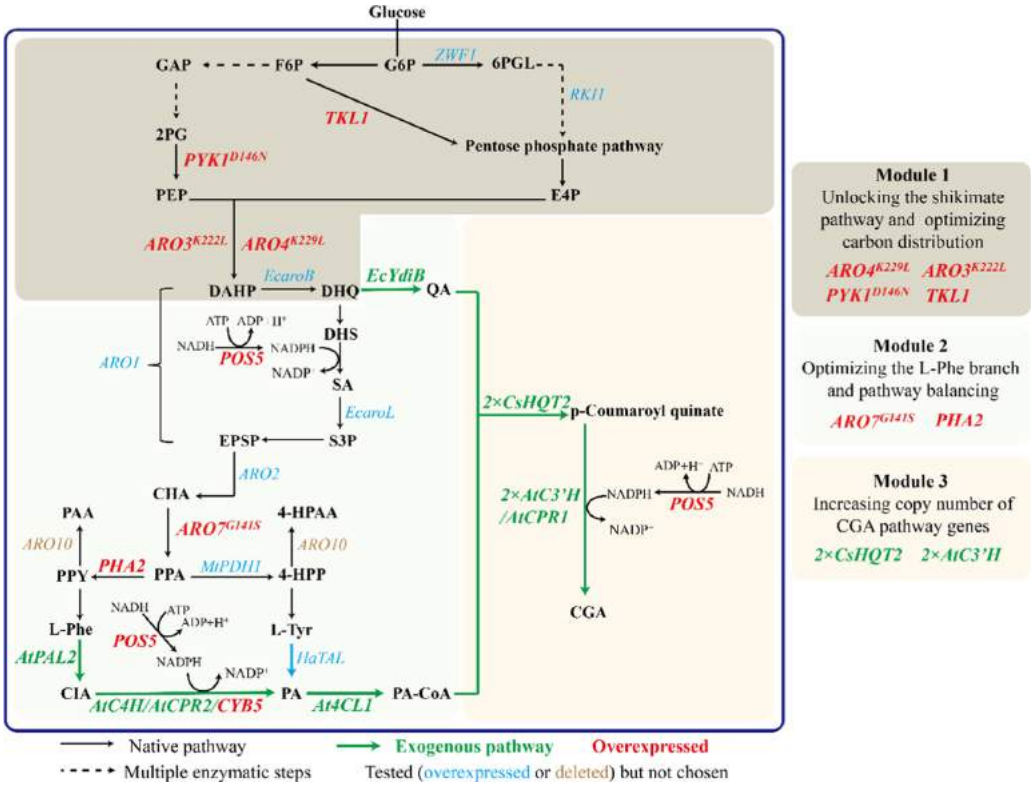

Figure 1. Schematic representation of the modular engineering strategy for high-level CGA production in *Saccharomyces cerevisiae*. An optimized CGA biosynthesis pathway was reconstituted, by employing *AtPAL2*, *AtC4H*, *At4CL1*, *AtC3′H*, *AtCPR1*, *AtCPR2*, *CsHQT2*, *EcYdiB*, and *CYB5*. Modular engineering strategy consists of unlocking the shikimate pathway and optimizing carbon distribution (Module 1), optimizing the L-Phe branch and pathway balancing (Module 2), and increasing copy number of CGA pathway genes (Module 3). Black arrows represent the native pathways; dashed arrows represent multiple enzymatic steps; green arrows (or genes) represent exogenous pathways (or genes); overexpressed genes are highlighted in red; overexpressed genes in blue and deleting gene *ARO10* in brown indicate that these genes were tested but not chosen. Metabolite abbreviations: G6P, glucose-6-phosphate; 6PGL, 6-phospho-D-glucono-1,5-lactone; F6P, fructose-6-phosphate; GAP, glycerin-aldehyde-3-phosphate; 2PG, 2-phospho-D-glycerate; PEP, phosphoenolpyruvate; E4P, erythose-4-phosphate; DAHP, 3-deoxy-D-arabino-heptulosonate-7-phosphate; DHQ, 3-dehydroquinate; DHS, 3-dehydro-shikimate; SA, shikimate; S3P, shikimate-3-phosphate; EPSP, 5-enolpyruvyl-shikimate-3-phosphate; CHA, chorismate; PPA, prephenate; PAA, phenylacetaldehyde; PPY, phenylpyruvate; 4-HPP, 4-hydroxy-phenylpyruvate; 4-HPAA, 4-hydroxy-phenylacetaldehyde; L-Phe, phenylalanine; L-Tyr, tyrosine; CIA, cinnamic acid; QA, quinic acid; PA, *p*-coumaric acid; CGA, chlorogenic acid. Gene abbreviations: *AtPAL2*, phenylalanine ammonia lyase 2; *AtC4H*, cinnamate-4-hydroxylase; *At4CL1*, 4-coumarate:CoA ligase 1; *AtC3′H*, cytochrome P450 98A3; *AtCPR1* and *AtCPR2*, P450 reductase; *CsHQT2*, hydroxycinnamoyl-CoA quinate transferase 2; *EcYdiB*, quinate/shikimate dehydrogenase; $ARO3^{K222L}$, L-phenylalanine feedback-insensitive DAHP synthase; $ARO4^{K229L}$, L-tyrosine feedback-insensitive DAHP synthase; $ARO7^{G141S}$, L-tyrosine feedback-insensitive chorismate mutase; $PYK1^{D146N}$, pyruvate kinase 1 mutant with reduced catalytic activity. Host abbreviations: *At*, *Arabidopsis thaliana*; *Cs*, *Cynara scolymus*; *Ec*, *Escherichia coli*. A full list of genes used in this study is provided in Table S1.

(Figure S1B), microbial 4-hydroxyphenylacetate 3-monooxygenase (HpaB) and its oxidoreductase (HpaC) catalyze the conversion of PA to CA[8−10] and HQT further catalyzes the condensation of caffeoyl-CoA and QA to form CGA. In route 2 (Figures 1 and S1B), HQT catalyzes *p*-coumaroyl-CoA and QA to synthesize *p*-coumaroyl quinate, which is subsequently hydroxylated to form CGA by a cytochrome P450 hydroxylase (C3′H).[11]

To date, several attempts have been made to achieve the biosynthesis of CGA by the esterification of QA and CA in engineered *E. coli*. In *E. coli*, only a small fraction of DHQ is converted into QA by quinate/shikimate dehydrogenase (YdiB), unless the 3-dehydroquinate dehydratase (AroD, converting DHQ to 3-dehydroshikimate (DHS)) encoding gene is deleted.[12] Unfortunately, the *aroD* deletion strain cannot synthesize PA and CA because the synthesis of aromatic amino acids including phenylalanine and tyrosine is blocked. Previously, CA[12] or the fermentation broth of another CA-producing strain[13] was supplemented. Alternatively, a polyculture system was designed consisting of three strains with each producing CA, QA, and CGA, respectively.[14] Accordingly, the production of CGA at titers as high as 450, 78, and 88.6 mg/L were reported. Although precursor addition or co-cultivation may be feasible approaches to minimize metabolic interference, the scalable production of CGA would be more feasible and cost-effective through the reconstitution of the whole biosynthetic pathway in a single strain using simple carbon sources (e.g., glucose).

Baker's yeast (*S. cerevisiae*) is a suitable chassis widely used to produce plant-derived natural products. In addition to advantages in genetic tractability, metabolic plasticity, and robustness for industrial-scale fermentation,[15−17] yeast also provides endomembrane structures and subcellular compartments for reconstitution of plant pathways with multiple

https://doi.org/10.1021/acssynbio.1c00487
ACS Synth. Biol. 2022, 11, 800−811

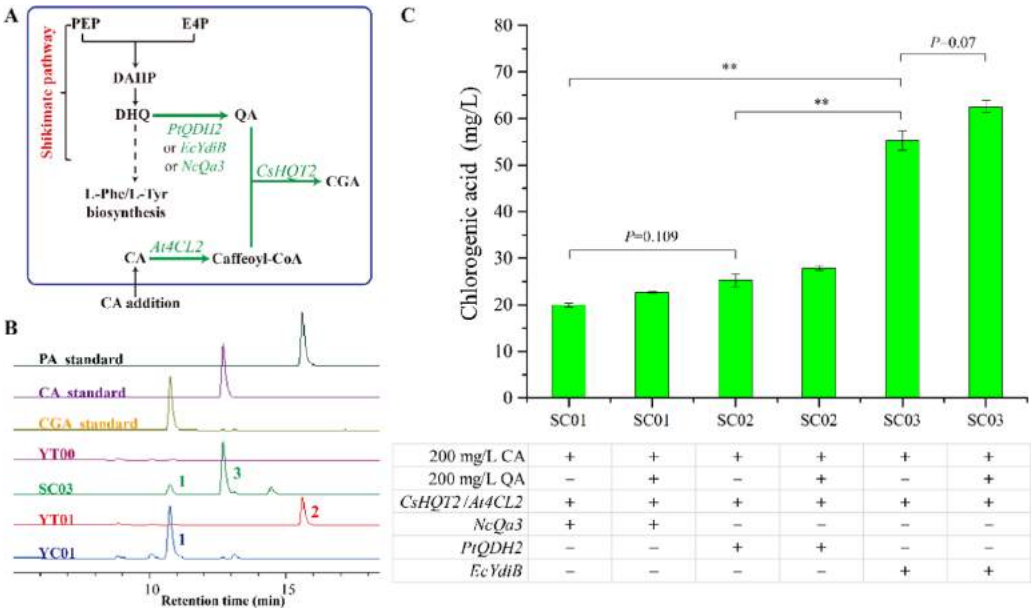

Figure 2. Exploration of *de novo* CGA biosynthesis in *S. cerevisiae*. (A) Schematic illustration of CGA biosynthesis in strain CEN.PK2-1C through plasmid-based overexpression of *EcYdiB*, *PtQDH2*, or *NcQa3*, together with *CsHQT2* and *At4CL2* under the condition of precursor CA addition. (B) HPLC profiles of standards CGA, CA, and PA, and samples from strains SC03, YT01, YC01, and YT00 (as control). Peak 1 corresponded to CGA, and peak 2 and peak 3 corresponded to PA and CA, respectively. HPLC chromatogram of SC03 is supplemented in Figure S3B. (C) Production of CGA in recombinant yeast strains. SC01, SC02, and SC03 were cultured in SC-Leu-His medium with 200 mg/L CA addition. QA (200 mg/L) was added to investigate its effect on CGA production. Average ± standard deviations were calculated from three biological replicates (*P < 0.05, **P < 0.01).

cytochrome P450 enzymes that are difficult to express in bacteria.[18,19] With the recent advances of functional genomics, metabolic engineering, and systematic and synthetic biology, many valuable shikimate pathway derivatives such as the nylon precursor muconic acid,[20,21] the flavoring agent vanillin,[22] and plenty of plant-sourced alkaloids[23−25] and flavonoids[26−28] have been synthesized in *S. cerevisiae*. The *de novo* biosynthesis of CGA in *S. cerevisiae* has not been previously reported, although a similar phenolic compound *p*-coumaroyl shikimate was produced in *S. cerevisiae* at a very low titer (1.6 mg/L) even with precursor PA addition.[29]

Therefore, the present work aimed to reconstitute a *de novo* CGA biosynthesis pathway in *S. cerevisiae*. Three traditional metabolic engineering modules were systematically optimized for improving CGA production including: (1) unlocking the shikimate pathway and optimizing carbon distribution; (2) optimizing and balancing branch pathways; and (3) increasing the copy number of CGA pathway genes. Finally, the engineered *S. cerevisiae* strain was able to produce CGA at a titer of 234.8 ± 11.1 mg/L in shake flasks and 806.8 ± 1.7 mg/L in a 1 L fed-batch fermenter, respectively.

RESULTS AND DISCUSSION

Exploration of CGA Biosynthesis in *S. cerevisiae* and Determination of Optimal Quinate Dehydrogenase. There are two diverging key precursors for the biosynthesis of CGA, PA derived from SA and QA derived from SA intermediate 3-dehydroquinate (DHQ) (Figure 1). The production of PA in yeast can be accomplished through a single heterologous enzymatic step from tyrosine or through two enzymatic steps from phenylalanine (Figure 1). However, the production of QA diverted from the SA pathway in yeast has not yet been reported, although many quinate dehydrogenases have been identified in bacteria, fungi, and plants.

Three quinate dehydrogenases EcYdiB, from *E. coli*, PtQDH2 from *Populus trichocarpa*, and NcQa3 from *Neurospora crassa*, were overexpressed together with At4CL2 from *A. thaliana* and CsHQT2 from *C. scolymus* (due to its high specificity and affinity for QA over SA[30]), to investigate the feasibility of CGA biosynthesis in *S. cerevisiae* (Figure 2A). Relevant plasmids were constructed and co-transformed into wild-type yeast CEN.PK2-1C to obtain the engineered strains SC01, SC02, and SC03, respectively (Table 1). Strains were cultured in SC medium supplemented with 200 mg/L CA. In addition, 200 mg/L QA was added to investigate its effect on CGA production. As shown in Figures 2B and S3A, a new compound peak (peak 1), with an identical retention time as CGA standard, was detected in three recombinant strains (SC01, SC02, and SC03), but not the control strain YT00. This new compound (peak 1) was further confirmed as CGA by LC-MS analysis (Figure S4B). Strain SC03 (EcYdiB) resulted in 55.3 ± 2.1 mg/L CGA production, 2.7-fold and 2.2-fold higher than SC01 (NcQa3, 19.9 ± 0.4 mg/L CGA) and SC02 (CsQDH2, 25.3 ± 1.5 mg/L CGA), respectively (Figure 2C). In addition, QA supplementation only slightly increased the production of CGA in strain SC03 (EcYdiB, P = 0.07). These results demonstrated that quinate dehydrogenase EcYdiB from *E. coli* was the optimal candidate for diverting the SA pathway intermediate to QA, and it is feasible to construct an artificial pathway for CGA biosynthesis in *S. cerevisiae*.

Engineering *p*-Coumaric Acid Biosynthesis from Phenylalanine. A previous study demonstrated that the phenylalanine branch produced much more PA than the

https://doi.org/10.1021/acssynbio.1c00487
ACS Synth. Biol. 2022, 11, 800−811

Table 1. Yeast Strains Used or Constructed in This Study

strain name	genotype/description	source
CEN.PK2-1C	*MATa; ura3-52; trp1-289; leu2-3112; his3Δ1; MAL2-8^{C}; SUC2*	our lab
SC01	CEN.PK2-1C/p413-CsHQT2-At4CL2, pH5-NcQa3	this study
SC02	CEN.PK2-1C/p413-CsHQT2-At4CL2, pH5-PtQDH2	this study
SC03	CEN.PK2-1C/p413-CsHQT2-At4CL2, pH5-EcYdiB	this study
YT00	CEN.PK2-1C, *IX1::TEF1p-spCas9-ADH2t*	this study
YT01	YT00, *XII2::(GPM1p-AtPAL2-ADH1t)-(GPDp-AtC4H-CYC1t)*	this study
YT02	YT01, *XI3::(ADH1t-CYB5-PGK1p)-(HXT7p-AtCPR2-CYC1t)*	this study
YC01	YT02, *X3::(GPDp-AtCPR1-CYC1t)-(ENO2p-CsHQT2-PGK1t)- (TPI1p-AtC3′H-TPI1t)-(TEF1p-EcYdiB-TEF1t)-(PGK1p-At4CL1-HXT7t)-HIS3*	this study
YC02	YC01, Δ*trp1::TEF1p-ARO4^{K229L}-CYC1t*	this study
YC03	YC02, Δ*ho-1::TPI1p-ARO3^{K222L}-TPI1t*	this study
YC04	YC02, Δ*ho-1::(HXT7t-EcAroB-PGKp)-(TPI1p-ARO3^{K222L}-TPI1t)*	this study
YC05	YC02, Δ*ho-1::(HXT7t-ARO7^{G141S}-PGK1p)-(TPI1p-ARO3^{K222L}-TPI1t)*	this study
YC06	YC05, Δ*ho-2::LEU2-(PDC1p-EcAroL-ADH3t)*	this study
YC07	YC06, *III1::(GPM1p-PHA2-ADH1t)-URA3*	this study
YC08	YC07, *XII5::GPDp-ARO2-CYC1t*	this study
YC09	YC07, *ARO1p::(GPDp-ARO2-CYC1t)-ENO2p*	this study
YC0701	YC05, *III1::(GPM1p-PHA2-ADH1t)-URA3*	this study
YC10	YC0701, Δ*YPR003C::GPDp-HaTAL-CPS1t*	this study
YC11	Y10, *X2::FBA1p-MtPDH1-CYC1t*	this study
YC12	YC11, Δ*aro10*	this study
YC13	YC12, *XII5::PGK1p-TKL1-HXT7t*	this study
YC14	YC12, *XII5::(PGK1t-RKI1-ENO2p)-(PGK1p-TKL1-HXT7t)*	this study
YC15	YC14, Δ*aro10-2::LEU2-(TPI1p-ZWF1-CYC1t)*	this study
YC0702	YC0701, *pyk1::PYK1^{D146N}*	this study
YC0703	YC0702, *XII5::PGK1p-TKL1-HXT7t*	this study
YC0704	YC0703, Δ*ho-2::GPDp-POS5-ADH1t*	this study
YC0705	YC0704, *X2::(TPI1p-AtC3′H-TPI1t)-TRP1*	this study
YC0706	YC0704, *X2::LEU2-(ENO2p-CsHQT2-PGK1t)*	this study
YC0707	YC0704, *X2::LEU2-(ENO2p-CsHQT2-PGK1t)-(TPI1p-AtC3′H-TPI1t)-TRP1*	this study

tyrosine branch in *S. cerevisiae*.[31] Therefore, phenylalanine ammonia lyase (AtPAL2) and cinnamic acid hydroxylase (AtC4H) were introduced first into yeast (Figure 3). The resultant strain YT01 was able to produce 9.9 ± 0.4 mg/L PA in mineral medium (Figure 3), and the HPLC profile is shown in Figure 2B (peak 2). As C4H is a membrane-associated plant-derived P450 enzyme, a previous study reported that the activity of C4H was significantly enhanced when cytochrome P450 reductase (AtCPR2) together with yeast native cytochrome b5 (CYB5) were overexpressed.[31] Accordingly, PA titer was further increased to 20.7 ± 0.2 mg/L in YT02 (Figure 3).

Reconstruction of the *De Novo* CGA Biosynthesis Pathway from Glucose without Precursor Addition. Next, a quinate dehydrogenase (EcYdiB), a hydroxycinnamoyl-CoA quinate transferase (CsHQT2), a *p*-coumarate 3′-hydroxylase (AtC3′H) together with a cytochrome P450 reductase (AtCPR1), and a 4-coumarate-CoA ligase 1 (At4CL1) were further introduced into the PA-producing strain YT02. HPLC analysis showed that a new compound (peak 1, Figure 2B) with identical retention time as CGA standard was detected in YC01 and the PA peak (peak 2, Figure 2B) disappeared. Peak 1 of YC01 was further analyzed by LC-MS to confirm the identity of this compound. Two noticeable ion peaks appeared at m/z 377.22 $(M + Na)^+$ and 355.13 $(M + H)^+$, consistent with the molecular weight (MW) of CGA (MW = 354.31) (Figure S4C). As shown in Figure 3, 36.6 ± 2.4 mg/L CGA was produced in strain YC01.

Unlocking the Carbon Flux into the Shikimic Acid Pathway for Improved CGA Production. It is important to increase the substrate flux into the shikimic acid (SA) pathway to enhance CGA production. The two isomeric DAHP synthases ARO3 and ARO4, which catalyze the entrance reaction into the SA pathway, are known to be feedback inhibited by the downstream aromatic amino acids.[32] Therefore, to maximize the carbon flux entering the SA pathway, two variants of *ARO4^{K229L}* and *ARO3^{K222L}* were overexpressed in *S. cerevisiae*, both of which were reported to be able to efficiently relieve feedback inhibition and increase the production of SA pathway derivatives such as PA,[31,33] muconic acid,[20,21] phenylethanol,[34] salidroside,[35] resveratrol,[36,37] and naringenin.[38,39] Indeed, the overexpression of *ARO4^{K229L}* (YC02) increased the production of CGA to 51.7 ± 1.4 mg/L, while further overexpression of *ARO3^{K222L}* (YC03) led to the production of 54.5 ± 0.7 mg/L CGA (Figure 3). Although the *E. coli* dehydroquinate synthase from (EcAroB) has previously been shown to be beneficial for the production of shikimate-derived chemicals such as PA,[33] the introduction of *EcAroB* (YC04) had no effect on CGA production in the present study (Figure 3).

Manipulating the L-Phenylalanine Branch and L-Tyrosine Branch for CGA Production. In the nonlinear CGA biosynthesis pathway, DHQ was the initial branchpoint and catalyzed into two diverging key precursors, PA and QA. PA (200 mg/L) or QA (200 mg/L) was added into the mineral medium to investigate the limited precursor in strain YC03. As shown in Figure 4A, the addition of PA greatly increased CGA production to 149.2 ± 4.0 mg/L, while the addition of QA resulted in a marginal increase in CGA titer (54.6 ± 1.5 mg/L). Therefore, PA is the key limited precursor for CGA biosynthesis in strain YC03.

Previous studies showed that the chorismate mutase mutant ARO7^{G141S} could efficiently relieve feedback inhibition by L-tyrosine and increase the metabolic flux from chorismate toward the L-tyrosine and L-phenylalanine branch.[31,40] Indeed, overexpression of *ARO7^{G141S}* (YC05) resulted in the production of 71.8 ± 1.8 mg/L CGA (Figure 4B), 32% higher than that of the parent strain YC03 ($P < 0.01$). Next, overexpression of the *E. coli* shikimate kinase (EcAroL), endogenous prephenate dehydratase (PHA2), chorismate synthase (ARO2), and pentafunctional aromatic protein

https://doi.org/10.1021/acssynbio.1c00487
ACS Synth. Biol. 2022, 11, 800−811

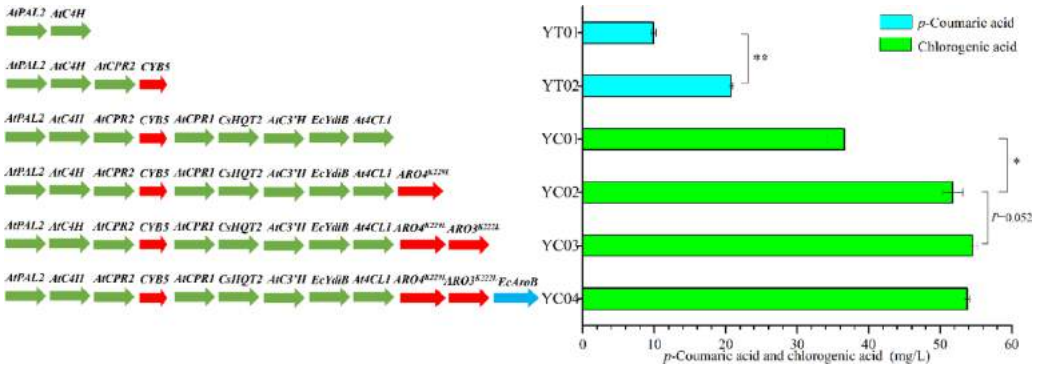

Figure 3. Reconstruction of a *de novo* CGA biosynthesis pathway in *S. cerevisiae*. Production of PA upon engineering *S. cerevisiae* L-phenylalanine pathway by overexpressing *AtPAL2* and *AtC4H*, and enhancement of P450 *AtC4H* activity by the functional expression of *AtCPR2* and *CYB5*. *At4CL1*, *EcYdiB*, *CsHQT2*, *AtC3′H*, and *AtCPR1* were further introduced to enable *de novo* CGA biosynthesis in *S. cerevisiae*. Then, $ARO4^{K229L}$, $ARO3^{K222L}$, and *EcAroB* were overexpressed to evaluate their effects on CGA production. The production of PA in YC01, YC02, YC03, and YC04 was lower than 0.5 mg/L and is provided in Figure S5. The displayed average values and standard deviations were calculated from three biological replicates (*$P < 0.05$, **$P < 0.01$).

(ARO1), which have previously been shown to be beneficial for the production of PA,[31] were systematically investigated. Unfortunately, the production of CGA in YC06, YC07, YC08, and YC09 decreased to 32.2 ± 2.0, 45.0 ± 0.9, 23.5 ± 0.7, and 3.6 ± 0.1 mg/L, respectively (Figure 4B). While the overexpression of *PHA2* seemed to have a positive impact on CGA production, the overexpression of *EcAroL*, *ARO2*, and *ARO1* significantly decreased CGA production (Figure 4B), probably due to the disturbance of the flux between PA and QA. Thus, YC0701 was constructed by individually overexpressing *PHA2*, which produced 93.1 ± 2.8 mg/L CGA (Figure 4B), representing a 30% improvement in CGA production compared with parent strain YC05 ($P < 0.01$). Meanwhile, only 0.6 mg/L PA was detected in strain YC0701 by the overexpression of *PHA2* (Figure S5), indicating the high efficiency of the downstream CGA conversion pathway.

The L-tyrosine branch was engineered by introducing L-tyrosine ammonia lyase from *Hemiphyllodactylus aurantiacus* (HaTAL) to further increase the flux toward PA in strain YC0701 (Figure 1). The resultant strain YC10 produced 90.4 ± 0.8 mg/L CGA, which displayed a slightly negative effect on CGA production (Figure 4B). Furthermore, L-tyrosine prephenate dehydrogenase from *Medicago truncatula* (MtPDH1) was overexpressed to remove the bottleneck in metabolic flux towards PA in the L-tyrosine branch, and the resultant strain YC11 only produced 87.8 ± 1.6 mg/L CGA, with no PA (<0.2 mg/L) accumulation (Figure S5). The combination of the L-tyrosine branch with the L-phenylalanine branch failed to further improve PA and CGA production. The knockout of *ARO10* was previously reported to improve the production of PA,[33] resveratrol,[37] and naringenin,[38] by reducing byproduct (aromatic alcohols) formation and directing the pathway flux to aromatic amino acids. Unexpectedly, the resultant strain YC12 decreased CGA production by 30% (Figure 4B), although a higher PA production (5.7 ± 0.1 mg/L) and higher biomass were observed (Figure S5). These results indicate that the metabolic flux between PA and QA needs to be carefully balanced to achieve optimal production of CGA.

Upstream Manipulations for Increased Precursor Availability. The SA pathway is initiated by the condensation of the two metabolite precursors, phosphoenolpyruvate (PEP) and erythrose-4-phosphate (E4P). The latter is considered as rate-limiting in the SA pathway in *S. cerevisiae*.[41] Thus, the next level of engineering was directed toward increasing the availability of E4P (Figure 1). The overexpression of transketolase (TKL1), ribose-5-phosphate ketol-isomerase (RKI1), and glucose-6-phosphate dehydrogenase (ZWF1) was investigated in strain YC12 (Figure 1), all of which have previously been implemented to increase the availability of E4P.[34,42−44] The resultant strains, YC13, YC14, and YC15, produced 65.2 ± 4.4, 62.7 ± 1.4, and 37.3 ± 0.2 mg/L CGA, respectively (Figure S6). The overexpression of *TKL1* (strain YC13) led to a slight increase in CGA production (65.2 ± 4.4 mg/L), the overexpression of *RKI1* (strain YC14) had no effect on CGA production, and the overexpression of *ZWF1* (strain YC15) had a significant negative effect on CGA production (Figure S6).

To further augment E4P availability to initiate the SA pathway, pyruvate kinase (PYK1) could represent another potential target, which converts most of PEP into pyruvate. The tuning of the flux by expressing the mutant allele $PYK1^{D146N}$ has previously been shown to be a successful approach to increase the production of 2-phenylethanol in *S. cerevisiae*.[34] Thus, the variant allele of $PYK1^{D146N}$ was reconstructed in YC0701 by CRISPR guided *in vivo* directed mutagenesis (Figure 5). The resultant strain YC0702 rendered a significant increase in the titer of CGA to as high as 207.2 ± 4.2 mg/L (Figure 5), although exhibiting a 46.9% decrease in the maximum specific growth rate (0.165 ± 0.003 h^{-1} of YC0702 vs 0.311 ± 0.019 h^{-1} of YC0701) (Table S5). Subsequent overexpression of *TKL1* resulted in the construction of strain YC0703, which produced 218.1 ± 2.4 mg/L CGA (Figure 5).

CGA biosynthesis requires a considerable amount of NADPH as a cofactor for P450 enzymes, AtC4H and AtC3′H.[45] Previous studies showed that the overexpression of *POS5* to enhance cofactor NADPH supply could significantly improve the production of noscapine[46] and lycopene.[47] Therefore, *POS5* was overexpressed in the best-performing strain YC0703 to promote the intracellular generation of NADPH for optimizing CGA biosynthesis. Unfortunately, the production of CGA (220.2 ± 4.6 mg/L) (Figure 5) was only marginally increased.

https://doi.org/10.1021/acssynbio.1c00487
ACS Synth. Biol. 2022, 11, 800−811

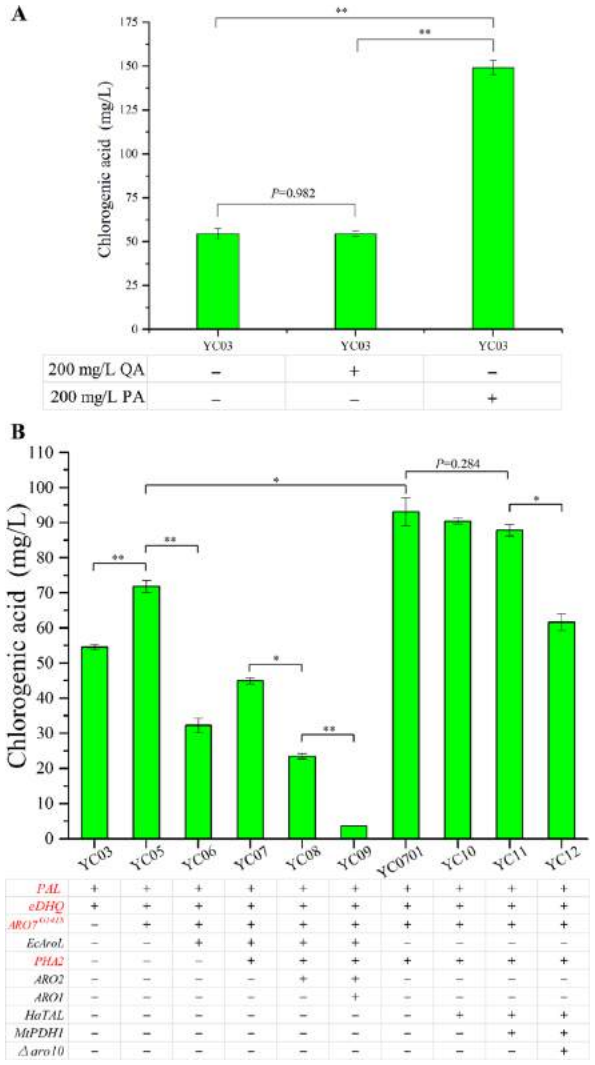

Figure 4. Optimization of the L-phenylalanine and L-tyrosine branch for CGA production. (A) Determination of the limiting precursors for CGA production. PA or QA (200 mg/L) was added to investigate their effects on CGA production in strain YC03. (B) Improving CGA production by optimizing the L-phenylalanine and L-tyrosine branch. *AtPAL2*, *AtC4H*, *At4CL1*, *EcYdiB*, *CsHQT2*, *AtC3′H*, *AtCPR1*, *AtCPR2*, and *CYB5* (named *PAL*) were introduced into yeast for CGA production. *eDHQ* represents upstream CGA-beneficial manipulations $ARO4^{K229L}$ and $ARO3^{K222L}$. In the L-phenylalanine biosynthesis pathway, overexpression of genes $ARO7^{G141S}$ and *PHA2* improved CGA production, while the overexpression of upstream genes *EcAroL*, *ARO2*, and *ARO1* severely influenced the CGA level. Overexpression of tyrosine ammonia lyase (HaTAL) and tyrosine prephenate dehydrogenase (MtPDH1) slightly decreased CGA production. Blocking competing pathways by *ARO10* deletion failed to improve CGA production. Genes marked in red indicate that overexpression of these genes was beneficial for CGA production. The displayed average values and standard deviations were calculated from three biological replicates (*P < 0.05, **P < 0.01).

Optimizing CGA Biosynthesis by Adjusting the Copy Number of CGA Biosynthesis Genes. Increasing the copy number of heterologous genes is a commonly employed strategy for pathway optimization. Thus, another copy of CGA biosynthesis pathway genes *AtC3′H* and *CsHQT2* integrated into YC0704 resulted in the construction of YC0705, YC0706, and YC0707. Compared with the parent strain YC0704 (220.2 ± 4.6 mg/L), YC0705, YC0706, and YC0707 produced 220.4 ± 2.9, 227.0 ± 9.2, and 234.8 ± 11.1 mg/L CGA, respectively (Figure 5). While individual integration of another copy of *AtC3′H* (YC0705) or *CsHQT2* (YC0706) led to no, or a slight, increase (3.1%) in CGA production, simultaneous integration of *AtC3′H* and *CsHQT2* (YC0707) enabled a modest improvement (6.6%) in CGA production (Figure 5).

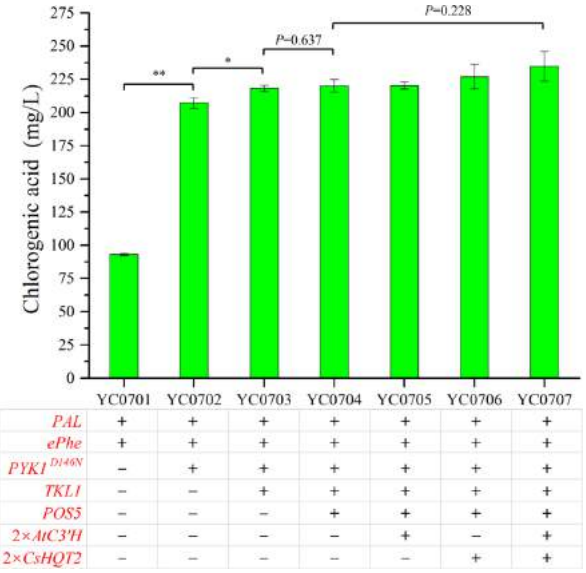

Figure 5. Optimization of carbon distribution and increase of pathway gene copy number for improved CGA production. The down-tuning of the catalytic activity of the pyruvate kinase ($PYK1^{D146N}$) increased precursor availability and significantly improved CGA production. The *PAL* consisting of *AtPAL2*, *AtC4H*, *At4CL1*, *EcYdiB*, *CsHQT2*, *AtC3′H*, *AtCPR1*, *AtCPR2*, and *CYB5* was employed for CGA production in yeast. *ePhe* represents the combination of upstream CGA-beneficial manipulations $ARO4^{K229L}$, $ARO3^{K222L}$, $ARO7^{G141S}$, and *PHA2*. Genes marked in red indicate that overexpression of these genes were beneficial for CGA production. The displayed average values and standard deviations were calculated from three biological replicates (*P < 0.05, **P < 0.01).

Production of CGA in Fed-Batch Fermentation. After optimizing the three modules for CGA biosynthesis (Figure 6A), the final engineered strain YC0707 produced CGA with a titer as high as 234.8 ± 11.1 mg/L in shake flasks, representing a 6.4-fold increase compared with the starting strain YC01 (Figure 6A). Fed-batch fermentation was performed in a 1 L fed-batch bioreactor, with an initial working volume of 0.5 L, to further promote CGA production. After the initial glucose (25 g/L) was consumed, a carbon restriction strategy was employed, with the glucose concentration maintained at 0.1−1 g/L by adjusting the feeding rate (Figure 6B). Cell densities were steadily increased, and OD_{660} reached a maximum of 54.6 after 59 h cultivation, while the production of CGA continued to increase and finally reached a titer of 806.8 mg/L after 70.5 h with a yield of 12.8 mg/g glucose (Figure 6B).

A comparison of metabolic engineering strategies to produce CGA and other SA derivatives in *S. cerevisiae* is summarized in Table 2. The overexpression of $ARO4^{K229L}$, $ARO3^{K222L}$, *TKL1*, $PYK1^{D146N}$, $ARO7^{G141S}$, and *PHA2* improved the production of

https://doi.org/10.1021/acssynbio.1c00487
ACS Synth. Biol. 2022, 11, 800−811

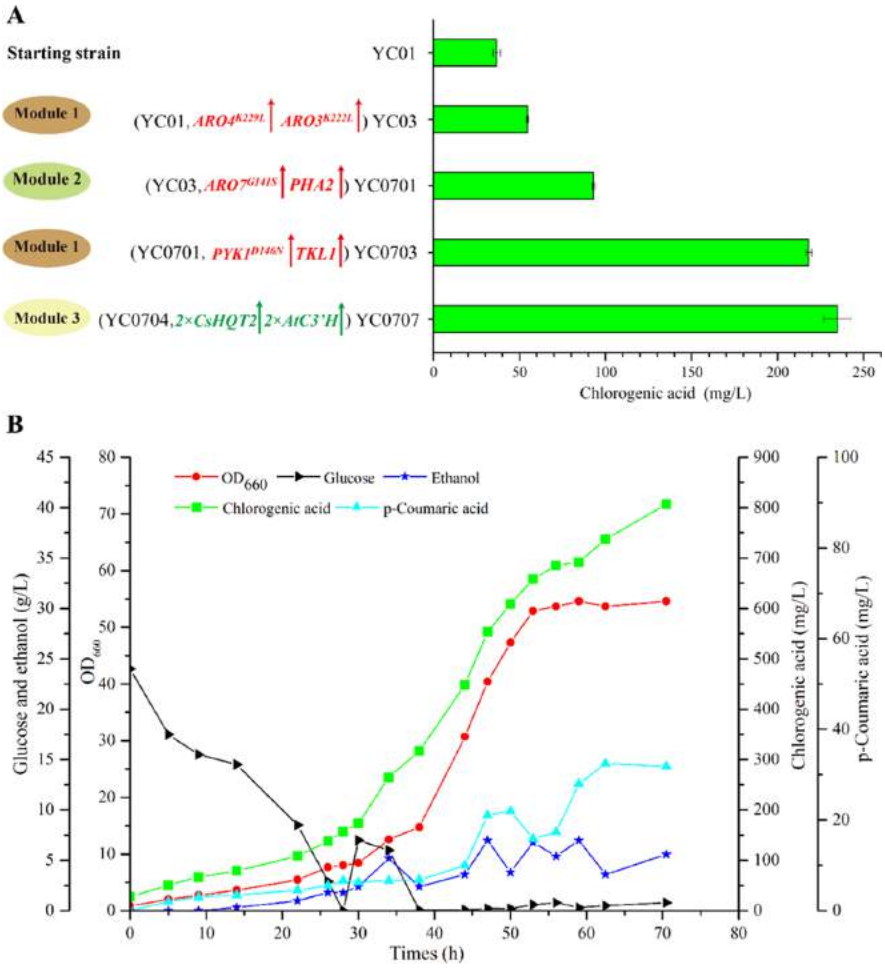

Figure 6. Increasing CGA production via modular pathway optimization and fed-batch fermentation. (A) CGA production in the engineered yeast strains using stepwise modular engineering strategy. (B) CGA production in YC0707 with fed-batch fermentation.

CGA and other SA derivatives, indicating the high consistency of metabolic engineering strategies for increasing the metabolic flux into the SA pathway. However, the genes underlined (Table 2), reported to be beneficial to produce SA derivatives in previous studies, were not helpful for CGA biosynthesis in the present study, probably due to the complexity of CGA downstream decoration steps involving a nonlinear biosynthetic pathway. Therefore, more metabolic engineering and pathway engineering efforts need to be employed to further optimize CGA biosynthesis in *S. cerevisiae*. For example, the expression level of rate-limiting enzymes of the SA pathway needs to be carefully regulated to control the flux into two competitive precursors, QA and PA. While the overexpression of *POS5* failed to increase CGA production, alternative strategies to improve NADPH supply[49] may contribute positively to the production of CGA. In addition, as the CGA biosynthetic pathway consists of cytochrome P450 enzymes (AtC3′H and AtC4H), strategies to expand endoplasmic reticulum membranes[50] (such as *PAH1* deletion and *ICE2* overexpression) should be evaluated for CGA biosynthesis in the near future. Moreover, bioprocess optimization should be performed to maximize the titer of CGA in *S. cerevisiae* for industrial applications.

CONCLUSIONS

There is an increasing demand for CGA in the food and pharmaceutical industries. The present study is the first to report the *de novo* CGA biosynthesis in *S. cerevisiae*. Using the multimodular engineering strategy, the best-performing strain was able to produce CGA at a titer of 234.8 ± 11.1 mg/L in shake flasks and 806.8 ± 1.7 mg/L in a 1 L fed-batch fermenter, respectively. This study opens a route to produce CGA from glucose in *S. cerevisiae* and establishes a platform for the biosynthesis of CGA-derived value-added products.

MATERIALS AND METHODS

Strains, Plasmids, and Chemicals. *E. coli* DH5α was used for the construction and propagation of all plasmids. *S. cerevisiae* CEN.PK2-1C (*MATa*; *ura3-52*; *trp1-289*; *leu2-3112*; *his3Δ1*; *MAL2-8*^{C}; *SUC2*) was used as the host for genome engineering and CGA production. All engineered strains and plasmids used in this work are listed in Tables 1 and S2, respectively. All genes used in this work are listed in Table S1, of which *CsHQT2* (from *C. scolymus*), *PtQDH2* (from *P. trichocarpa*), *NcQa3* (from *N. crassa*), and *MtPDH1* (from *M. truncatula*) were codon-optimized and synthesized at Generay

https://doi.org/10.1021/acssynbio.1c00487
ACS Synth. Biol. 2022, 11, 800−811

Table 2. Comparison of Metabolic Engineering Strategies between CGA and Other SA Derivatives Engineered in *S. cerevisiae*[ab]

representative product		metabolic engineering strategies	titer (g/L)	reference
upstream products from the SA pathway	muconic acid	pathway genes (*CaHQD2*, *PaAroZ*, *KpAroY*), *degron-tagged ARO1*(*ARO1-Cln2*$_{PEST}$), *ARO4*^{K229L}, *TKL1*, *EcAroB*, *EcAroD*, *PAD1*, Δ*aro4*, Δ*aro3*	1.2 or 5.1 (addition of amino acid); Fed-batch bioreactor (168 h)	20
	shikimate	*ARO1*^{D920A}, *ARO4*^{K229L}, *TKL1*, *RKI1*, Δ*ric1*, Δ*aro1*	1.98 (glucose) or 2.5 (sucrose); Shake flask (72 h)	42
aromatic alcohols	2-phenylethanol	*ARO4*^{K229L}, *ARO3*^{K222L}, *TKL1*, *PYK1*^{D146N}, *EcAroL*, *ARO1*, *ARO2*, *ARO7*^{T226I}, *PHA2*, *ARO10*, *ARO9*, *tyr1p:YEN1p*, Δ*aro3*, Δ*aro8*	1.59; Fed-batch bioreactor (40 h)	34
phenylethanoids	salidroside	pathway genes (*4HPAAS*, *4HPAR*, *RrU8GT33*), *ARO4*^{K229L}, *ARO3*^{K222L}, *TKL1*, *RKI1*, *EcAroL*, *ARO1*, *ARO2*, *ARO7*^{G141S}, *ARO10*, *PGM1*, *UPG1*, Δ*pdc1*, Δ*pha2*, Δ*trp2*	26.55; Fed-batch bioreactor (168 h) (YPD)	35
stilbenoids	resveratrol	pathway genes (*HaTAL*, *At4CL1*, *VvVST1*), *ARO4*^{K229L}, *ARO7*^{G141S}, *ACC1*$^{S659A, S1157A}$, integration of multiple copies of *HaTAL*, *At4CL1*, and *VvVST1*	0.42 (glucose) or 0.53 (ethanol); Two-stage fed-batch bioreactor (100 h)	36
	resveratrol	pathway genes (2×*AtPAL2*, 2×*AtC4H*, 2×*At4CL2*, 2×*VvVST1*, *AtCPR2*, *CYB5*), *ARO4*^{K229L}, *ARO7*^{G141S}, *EcAroL*, *SeACS1*^{L641P}, *ACC1*$^{S659A, S1157A}$, Δ*aro10*	0.81; Fed-batch bioreactor (110 h)	37
flavonoids	naringenin	pathway genes (*RtTAL*, *AtC4H*, *At4CL1*, *HaCHS*) (plasmid-based overexpression)	0.007; Shake flask (40 h) (YPL)	48
	naringenin	pathway genes (*AtPAL1*, *AtC4H*, *RcTAL*, *At4CL3*, 2×*AtCHS3*, *AtCHI1*, *AtCPR1*), *ARO4*^{G226S}, Δ*aro3*, Δ*aro10*, Δ*pdc5*, Δ*pdc6*	0.22; Batch bioreactor (40 h)	38
phenylpropanoic acids	*p*-coumaric acid	pathway genes (*AtPAL2*, *AtC4H*, *FjTAL*, *AtCPR2*, *CYB5*), *ARO4*^{K229L}, *BbXfpk*, *EcAroL*, *ARO1*, *ARO2*, *ARO3*, *ARO7*^{G141S}, *PHA2*, *MtPDH1*, *CkPta*, *pfk1::(SET3p-PFK1)*, *pfk2::(CDC24p-PFK2)*, *pyk1::(ALD5p-PYK1)*, Δ*gal7/10/1*, Δ*gpp1*, Δ*gal80*, Δ*aro10*, Δ*pdc5*	12.5; Fed-batch bioreactor (96 h)	31
	caffeic acid	pathway genes (*RgTAL*, *PaHpaB*, *SeHpaC*), *ARO4*^{K229L}, *ARO7*^{G141S}, *ZmTyrC*, Δ*aro10*, Δ*aro3*, Δ*gal80*	0.57; Shake flask (72 h) (YPD)	10
	chlorogenic acid	pathway genes (*AtPAL2*, *AtC4H*, *At4CL1*, *EcYdiB*, 2×*CsHQT2*, 2×*AtC3′H*, *AtCPR1*, *AtCPR2*, *CYB5*), *ARO4*^{K229L}, *ARO3*^{K222L}, *TKL1*, *pyk1::PYK1*^{D146N}, *ARO7*^{G141S}, *PHA2*	0.8; Fed-batch bioreactor (70.5 h)	this study

[a]Genes underlined were reported to be beneficial for the production of SA derivative in previous studies, but not helpful for CGA biosynthesis in the present study. A schematic diagram of the biosynthetic pathways of these SA derivatives is shown in Figure S7. [b]Note: *ARO4*^{G226S} and *ARO7*^{T226I} are two feedback-insensitive variants parallel to *ARO4*^{K229L}and *ARO7*^{G141S}, respectively. And *HaTAL*, *RtTAL*, *RcTAL*, *FjTAL*, and *RgTAL* are five heterologous tyrosine ammonia lyase genes from *H. aurantiacus*, *Rhodosporidium toruloides*, *Rhodobacter capsulatus*, *Flavobacterium johnsoniaeu*, and *Rhodotorula glutinis*, respectively.

https://doi.org/10.1021/acssynbio.1c00487
ACS Synth. Biol. 2022, 11, 800−811

Biotech (Shanghai, China). All primers were synthesized by Tsingke Biotech (Hangzhou, China) and are listed in Table S3.

A Gibson assembly kit was purchased from New England Biolabs (Ipswich). PrimeStar DNA polymerase, restriction enzymes, and DNA ligase were purchased from TaKaRa Bio (Dalian, China). Plasmid miniprep and DNA purification kits were purchased from Thermo Fisher Scientific (Waltham). Genome extraction kit, RNA extraction kit, and reverse transcription kit were purchased from CWBIO (Jiangsu, China). The standards of quinic acid (QA), *p*-coumaric acid (PA), caffeic acid (CA), and chlorogenic acid (CGA) were purchased from Sigma-Aldrich (St. Louis). All chemical reagents not mentioned above were purchased from Sangon Biotech (Shanghai, China).

DNA Manipulation. All native promoters, genes, and terminators were PCR amplified from *S. cerevisiae* CEN.PK2-1C genomic DNA or the corresponding plasmids. For codon-optimized genes, including *CsHQT2*, *PtQDH2*, *NcQa3*, and *MtPDH1*, synthetic fragments (obtained from Generay Biotech) were used for PCR amplification. *At4CL1* (from *A. thaliana*) was amplified from the *A. thaliana* cDNA library. Codon-optimized *AtPAL2*, *AtC4H*, and *AtCPR2* as well as *CYB5* and *At4CL2* expression cassettes (*PGK1p-CYB5-ADH1t*; *PGK1p-At4CL2-ADH1t*) were amplified from pCfB2584 and pCfB2767.[37] Codon-optimized *HaTAL* (from *H. aurantiacus*) and *AtC3′H* with its P450 reductase gene *AtCPR1* were amplified from the plasmid pTAL[28] and pLC-c3,[51] respectively. *EcYdiB* and *EcAroL* were amplified from *E. coli* genomic DNA.

These candidate genes were cloned into the helper plasmids (pH1, pH2, pH3, pH4, pH5, pH6)[52] or assembled with the corresponding promoters and terminators into pUC19 using restriction-ligation or Gibson assembly. Furthermore, these expression cassettes were amplified and assembled into multiple-gene pathways using the DNA assembler method, which were integrated into selected genomic loci that have been demonstrated to provide stable and high-level expression.[53,54] All integration cassettes are listed in Table S3. All guide RNA (gRNA) plasmids were constructed by Gibson assembly using the corresponding primers pairs with the plasmid pKan100-ADE2.1[55] as the template. Guide RNAs (gRNAs) were designed on the E-CRISP website (http://www.e-crisp.org).[56] All gRNA sequences and target sites used in this study are listed in Table S4.

The mutant genes $ARO3^{K222L}$, $ARO4^{K229L}$, $ARO7^{G141S}$, and $PYK1^{D146N}$ were generated by overlapped extension PCR. To construct p413-CsHQT2-At4CL2, the *At4CL2* cassette (*PGK1p-At4CL2-ADH1t*) from pCfB2584 and *CsHQT2* cassette (*ENO2p-CsHQT2-PGK1t*) from pH3-CsHQT2 were cloned into p413 by Gibson assembly. To construct pUC19-AtCPR2-CYB5, four fragments, including *CYB5* cassette (*PGK1p-CYB5-ADH1t*) from pCfB2767, *HXT7* promoter (*HXT7p*), *AtCPR2*, and *CYC1* terminator (*CYC1t*), were cloned into pUC19 by Gibson assembly. To construct pUC19-EcAroL-LEU2, pUC19-ZWF1-LEU2, or pUC19-PHA2-URA3, four fragments, including the marker cassette, target gene, the corresponding promoter, and terminator, were amplified by PCR and circularized using Gibson assembly kit. To construct pH5-EcYdiB-HIS3, pH3-CsHQT2-LEU2, or pH4-AtC3′H-TRP1, the marker cassette was amplified and cloned into restriction site (*Sma*I, *Pst*I, or *Sac*II) of the corresponding plasmid (pH5-EcYdiB, pH3-CsHQT2, or pH4-AtC3′H) by Gibson assembly, respectively. All plasmid constructions are provided in Table S3.

Strain Construction. A previously described CRISPR/Cas9 system was adopted for gene deletion and site-specific integration in *S. cerevisiae*.[57] An overview of yeast strain genealogy in this study is provided in Figure S2. To facilitate genetic manipulation, a Cas9 expression cassette was amplified from p42H-spCas9 and integrated into *IX1* locus in *S. cerevisiae* CEN.PK2-1C, and the resultant strain YT00 (CEN.PK2-1C, *IX1::TEFp-spCas9-ADH2t*) was used as the host for subsequent DNA integration and biosynthetic pathway engineering. Then, equimolar amounts of purified linearized fragments (50−100 ng/kb) flanked by 40−60 bp homologous arms were co-transformed with the corresponding gRNA plasmid (∼300 to 500 ng) into *S. cerevisiae* using the LiAc/ssDNA/PEG method, and transformants were selected on YPD plates supplemented with 200 μg/L G418. Clones were verified by colony PCR using Green Taq Mix (Vazyme Biotech, Nanjing, China). Subsequently, these clones with correct module integration were cultivated overnight in YPD liquid medium and then streaked onto antibiotic-free plates to remove the gRNA plasmids.

Strain Cultivation. *E. coli* recombinant strains were cultured in LB medium containing 10 g/L tryptone, 5 g/L yeast extract, and 10 g/L NaCl, supplemented with 100 μg/mL ampicillin at 37 °C. Yeast strains for genetic manipulation were routinely cultivated in YPD medium containing 10 g/L yeast extract, 20 g/L peptone, and 20 g/L glucose, supplemented with 200 μg/mL G418 and/or 100 μg/mL hygromycin when necessary.

For choosing optimal quinate dehydrogenase and the exploration of the feasibility of CGA biosynthesis in *S. cerevisiae* (Figure 2A), single colonies of CEN.PK2-1C strain containing a *LEU2*-based plasmid pH5-EcYdiB, pH5-NcQa3, or pH5-PtQDH2, together with a *HIS3*-based plasmid p413-CsHQT2-At4CL2 were inoculated into 5 mL of SC-Leu-His medium (1.7 g/L yeast nitrogen base (YNB), 5 g/L $(NH_4)_2SO_4$, 20 g/L glucose, 20 mg/L uracil, and 20 mg/L L-tryptophan) at 30 °C and 220 rpm for 24 h. Then, 1 mL seed culture was inoculated into a 250 mL flask containing 50 mL of SC-Leu-His medium supplemented with 200 mg/L CA and cultured at 30 °C and 220 rpm for 72 h.

Shake flask batch fermentations for producing PA and CGA were performed in minimal medium (15 g/L $(NH_4)_2SO_4$, 8 g/L KH_2PO_4, 3 g/L $MgSO_4$, and 25 g/L glucose, 10 mL/L trace metal, and 12 mL/L vitamin solutions).[58,59] Single colonies of engineered yeast strains were picked into 5 mL of minimal medium and incubated at 30 °C and 220 rpm for 24 h. Precultures (∼1 mL) were then inoculated into a 250 mL flask containing 50 mL of minimal medium to an initial OD_{660} of 0.05 and incubated at 30 °C and 220 rpm for 72 h. When necessary, 150 mg/L uracil, 250 mg/L leucine, 75 mg/L tryptophan, and 125 mg/L histidine were supplemented into the minimal medium. For investigating the limited precursor of CGA biosynthesis in engineered yeast strain YC03, 200 mg/L PA and 200 mg/L QA were added to the minimal medium, respectively. All of the fermentation experiments were performed in biological triplicate.

Bioreactor Fermentation. A single colony of YC0707 was inoculated into 5 mL of minimal media and incubated at 30 °C and 220 rpm for 24 h. Then, 2 mL of seed culture (4%) was transferred into two 250 mL flasks each containing 50 mL of fresh minimal medium and grown for an additional 22 h. The

https://doi.org/10.1021/acssynbio.1c00487
ACS Synth. Biol. 2022, 11, 800−811

resulting cultures (100 mL) were transferred into a 1 L bioreactor (MiniBox 1L*4 Parallel Bioreactor System, T&J Bio-engineering (Shanghai) Co. Ltd, Shanghai, China) containing 0.5 L of minimal medium with an initial OD_{660} of 0.9. Fermentation in the bioreactor was conducted at 30 °C and 300−1000 rpm, with an air flow rate of 1 L/min to keep the DO above 40%, and the pH was maintained at 5.5 by the automatic addition of ammonium hydroxide. When the ethanol concentration dropped to below 3 g/L, the feeding solution containing 500 g/L glucose, 9.0 g/L KH_2PO_4, 2.5 g/L $MgSO_4$, 3.5 g/L K_2SO_4, 0.28 g/L Na_2SO_4, 10 mL/L trace elements solution, and 12 mL/L vitamin solution was fed into the bioreactor with a rate at 5.4−10.8 mL/h. Samples were taken at regular intervals to determine OD_{660} and CGA concentration.

Analytical Methods. To quantify PA, CA, and CGA, culture samples (600 μL) were mixed with an equal volume of ethanol (100% v/v), vortexed thoroughly, and centrifuged at 13 500*g* for 5 min. The supernatants were analyzed on an Agilent 1260 HPLC instrument equipped with a reversed-phase C18 column (250 × 4.6 mm^2, 5 μm; Agilent) and a UV detector operating at 30 °C with a flow rate of 1 mL/min. The compounds were separated by elution with solution A (methanol) and solution B (0.2% acetic acid in water) gradient program. The gradient program was set as follows: 0.00−15.00 min, 10−50% A in B; 15.00−16.00 min, 50−10% A in B; 16.00−25.00 min, 10% A in B. The injection volume was 10 μL. PA was detected at 308 nm (15.6 min), and CA and CGA were detected at 324 nm (12.7 and 10.7 min, respectively). The mass value of CGA was measured by a Thermo Ultimate 3000 HPLC system coupled with a mass spectrometer (Thermo, LTQ-XL) equipped with an electrospray ionization device (LC-MS). Confirmation of the identity of CGA was done by comparing the retention time and accurate mass spectrum with the standard. Cell concentration was monitored by measuring the optical density at 660 nm with a spectrophotometer. Yeast cells were harvested by centrifugation at 12 000 rpm for 2 min. The supernatant was used for glucose and ethanol analysis with a biosensor analyzer SBA-40D (Shandong, China).

■ ASSOCIATED CONTENT

Supporting Information

The Supporting Information is available free of charge at https://pubs.acs.org/doi/10.1021/acssynbio.1c00487.

> CGA biosynthetic pathways; flowchart for strain construction; HPLC analysis; mass spectra analysis; PA production and biomass accumulation; combinatorial strategy for improving CGA production; and biosynthetic pathways of representative SA derivatives (Figures S1−S7) and list of genes; list of plasmids; list of primers and DNA fragments; integrations sites used; and maximum growth rates of engineered strains (Tables S1−S5) (PDF)

■ AUTHOR INFORMATION

Corresponding Author

Weihong Zhong − *College of Biotechnology and Bioengineering, Zhejiang University of Technology, Hangzhou 310014, China;* orcid.org/0000-0002-5673-2222; Email: whzhong@zjut.edu.cn

Authors

Feng Xiao − *College of Biotechnology and Bioengineering, Zhejiang University of Technology, Hangzhou 310014, China; Key Laboratory of Biomass Chemical Engineering of Ministry of Education, College of Chemical and Biological Engineering, Zhejiang University, Hangzhou 310027, China; Hangzhou Global Scientific and Technological Innovation Center, Zhejiang University, Hangzhou 310027, China;* orcid.org/0000-0003-2770-7578

Jiazhang Lian − *Key Laboratory of Biomass Chemical Engineering of Ministry of Education, College of Chemical and Biological Engineering, Zhejiang University, Hangzhou 310027, China; Hangzhou Global Scientific and Technological Innovation Center, Zhejiang University, Hangzhou 310027, China;* orcid.org/0000-0001-9784-9876

Shuai Tu − *College of Biotechnology and Bioengineering, Zhejiang University of Technology, Hangzhou 310014, China*

Linlin Xie − *College of Biotechnology and Bioengineering, Zhejiang University of Technology, Hangzhou 310014, China*

Jun Li − *College of Biotechnology and Bioengineering, Zhejiang University of Technology, Hangzhou 310014, China;* orcid.org/0000-0003-3632-0041

Fuming Zhang − *Department of Chemical and Biological Engineering, Center for Biotechnology and Interdisciplinary Studies, Rensselaer Polytechnic Institute, Troy, New York 12180, United States;* orcid.org/0000-0003-2803-3704

Robert J. Linhardt − *Department of Chemical and Biological Engineering, Center for Biotechnology and Interdisciplinary Studies, Rensselaer Polytechnic Institute, Troy, New York 12180, United States;* orcid.org/0000-0003-2219-5833

Haichan Huang − *College of Biotechnology and Bioengineering, Zhejiang University of Technology, Hangzhou 310014, China*

Complete contact information is available at: https://pubs.acs.org/10.1021/acssynbio.1c00487

Author Contributions

F.X. contributed to conceptualization, methodology, validation, investigation, resources, writing—original draft, writing—review and editing, and visualization. J. Lian performed writing—review and editing and visualization. S.T. and L.X. carried out investigation. J. Li contributed to methodology. F.Z. and R.J.L. performed writing—review and editing. H.H. contributed to resources. W.Z. performed conceptualization, supervision, project administration, writing—review and editing, and funding acquisition.

Notes

The authors declare no competing financial interest.

■ ACKNOWLEDGMENTS

This work was financially supported by the National Key Research and Development Program of China (2021YFA0909500) and National Natural Science Foundation of China (no. 31970104). The authors thank Prof. Jens Nielsen (Chalmers University of Technology, Sweden) and Prof. Irina Borodina (Technical University of Denmark, Denmark) for sharing the plasmid pCfB2584 and pCfB2767. Prof. Mingqiang Qiao (Nankai University, China) and Prof.

Jiachen Zi (Jinan University, China) were also appreciated for sharing the plasmid pLC-c3 and pTAL, respectively.

■ ABBREVIATIONS

QA, quinic acid; PA, *p*-coumaric acid; CA, caffeic acid; CGA, chlorogenic acid; DHQ, 3-dehydroquinate; SA, shikimic acid

■ REFERENCES

(1) Upadhyay, R.; Mohan Rao, L. J. An outlook on chlorogenic acids-occurrence, chemistry, technology, and biological activities. *Crit. Rev. Food Sci. Nutr.* **2013**, *53*, 968−984.
(2) Liang, N.; Kitts, D. D. Role of chlorogenic acids in controlling oxidative and inflammatory stress conditions. *Nutrients* **2016**, *8*, No. 16.
(3) Naveed, M.; Hejazi, V.; Abbas, M.; Kamboh, A. A.; Khan, G. J.; Shumzaid, M.; Ahmad, F.; Babazadeh, D.; FangFang, X.; Modarresi-Ghazani, F.; WenHua, L.; XiaoHui, Z. Chlorogenic acid (CGA): A pharmacological review and call for further research. *Biomed. Pharmacother.* **2018**, *97*, 67−74.
(4) Tajik, N.; Tajik, M.; Mack, I.; Enck, P. The potential effects of chlorogenic acid, the main phenolic components in coffee, on health: a comprehensive review of the literature. *Eur. J. Nutr.* **2017**, *56*, 2215−2244.
(5) Santana-Gálvez, J.; Cisneros-Zevallos, L.; Jacobo-Velazquez, D. A. Chlorogenic acid: Recent advances on its dual role as a food additive and a nutraceutical against metabolic syndrome. *Molecules* **2017**, *22*, No. 358.
(6) Lu, H.; Tian, Z.; Cui, Y.; Liu, Z.; Ma, X. Chlorogenic acid: A comprehensive review of the dietary sources, processing effects, bioavailability, beneficial properties, mechanisms of action, and future directions. *Compr. Rev. Food Sci. Food Saf.* **2020**, *19*, 3130−3158.
(7) Niggeweg, R.; Michael, A. J.; Martin, C. Engineering plants with increased levels of the antioxidant chlorogenic acid. *Nat. Biotechnol.* **2004**, *22*, 746−754.
(8) Huang, Q.; Lin, Y.; Yan, Y. Caffeic acid production enhancement by engineering a phenylalanine over-producing *Escherichia coli* strain. *Biotechnol. Bioeng.* **2013**, *110*, 3188−3196.
(9) Liu, L.; Liu, H.; Zhang, W.; Yao, M.; Li, B.; Liu, D.; Yuan, Y. Engineering the biosynthesis of caffeic acid in *Saccharomyces cerevisiae* with heterologous enzyme combinations. *Engineering* **2019**, *5*, 287−295.
(10) Zhou, P.; Yue, C.; Shen, B.; Du, Y.; Xu, N.; Ye, L. Metabolic engineering of *Saccharomyces cerevisiae* for enhanced production of caffeic acid. *Appl. Microbiol. Biotechnol.* **2021**, *105*, 5809−5819.
(11) Schoch, G.; Goepfert, S.; Morant, M.; Hehn, A.; Meyer, D.; Ullmann, P.; Werck-Reichhart, D. CYP98A3 from *Arabidopsis thaliana* is a 3′-hydroxylase of phenolic esters, a missing link in the phenylpropanoid pathway. *J. Biol. Chem.* **2001**, *276*, 36566−36574.
(12) Kim, B. G.; Jung, W. D.; Mok, H.; Ahn, J. H. Production of hydroxycinnamoyl-shikimates and chlorogenic acid in *Escherichia coli* production of hydroxycinnamic acid conjugates. *Microb. Cell Fact.* **2013**, *12*, No. 15.
(13) Cha, M. N.; Kim, H. J.; Kim, B. G.; Ahn, J. H. Synthesis of chlorogenic acid and *p*-coumaroyl shikimates from glucose using engineered *Escherichia coli*. *J. Microbiol. Biotechnol.* **2014**, *24*, 1109−1117.
(14) Li, S.; Liang, C.; Liu, G.; Jin, J. M.; Tao, Y.; Tang, S. Y. *De novo* biosynthesis of chlorogenic acid using an artificial microbial community. *J. Agric. Food Chem.* **2021**, *69*, 2816−2825.
(15) Zhang, M.; Zhang, K.; Mehmood, M. A.; Zhao, Z. K.; Bai, F.; Zhao, X. Deletion of acetate transporter gene *ADY2* improved tolerance of *Saccharomyces cerevisiae* against multiple stresses and enhanced ethanol production in the presence of acetic acid. *Bioresour. Technol.* **2017**, *245*, 1461−1468.
(16) Zhang, M. M.; Zhao, X. Q.; Cheng, C.; Bai, F. W. Improved growth and ethanol fermentation of *Saccharomyces cerevisiae* in the presence of acetic acid by overexpression of *SETS* and *PPR1*. *Biotechnol. J.* **2015**, *10*, 1903−1911.
(17) Lian, J. Z.; Mishra, S.; Zhao, H. M. Recent advances in metabolic engineering of *Saccharomyces cerevisiae*: New tools and their applications. *Metab. Eng.* **2018**, *50*, 85−108.
(18) Borodina, I.; Nielsen, J. Advances in metabolic engineering of yeast *Saccharomyces cerevisiae* for production of chemicals. *Biotechnol. J.* **2014**, *9*, 609−620.
(19) Jiang, H.; Morgan, J. A. Optimization of an in vivo plant P450 monooxygenase system in *Saccharomyces cerevisiae*. *Biotechnol. Bioeng.* **2004**, *85*, 130−137.
(20) Pyne, M. E.; Narcross, L.; Melgar, M.; Kevvai, K.; Mookerjee, S.; Leite, G. B.; Martin, V. J. J. An engineered Aro1 protein degradation approach for increased *cis,cis*-muconic acid biosynthesis in *Saccharomyces cerevisiae*. *Appl. Environ. Microbiol.* **2018**, *84*, No. e01095-18.
(21) Brückner, C.; Oreb, M.; Kunze, G.; Boles, E.; Tripp, J. An expanded enzyme toolbox for production of *cis,cis*-muconic acid and other shikimate pathway derivatives in *Saccharomyces cerevisiae*. *FEMS Yeast Res.* **2018**, *18*, No. foy017.
(22) Brochado, A. R.; Matos, C.; Moller, B. L.; Hansen, J.; Mortensen, U. H.; Patil, K. R. Improved vanillin production in baker's yeast through in silico design. *Microb. Cell Fact.* **2010**, *9*, No. 84.
(23) Galanie, S.; Thodey, K.; Trenchard, I. J.; Filsinger Interrante, M.; Smolke, C. D. Complete biosynthesis of opioids in yeast. *Science* **2015**, *349*, 1095−1100.
(24) Ping, Y.; Li, X.; You, W.; Li, G.; Yang, M.; Wei, W.; Zhou, Z.; Xiao, Y. *De novo* production of the plant-derived tropine and pseudotropine in yeast. *ACS Synth. Biol.* **2019**, *8*, 1257−1262.
(25) Srinivasan, P.; Smolke, C. D. Engineering a microbial biosynthesis platform for *de novo* production of tropane alkaloids. *Nat. Commun.* **2019**, *10*, No. 3634.
(26) Rodriguez, A.; Strucko, T.; Stahlhut, S. G.; Kristensen, M.; Svenssen, D. K.; Forster, J.; Nielsen, J.; Borodina, I. Metabolic engineering of yeast for fermentative production of flavonoids. *Bioresour. Technol.* **2017**, *245*, 1645−1654.
(27) Chen, R.; Yang, S.; Zhang, L.; Zhou, Y. J. Advanced strategies for production of natural products in yeast. *iScience* **2020**, *23*, No. 100879.
(28) Yang, J.; Liang, J.; Shao, L.; Liu, L.; Gao, K.; Zhang, J. L.; Sun, Z.; Xu, W.; Lin, P.; Yu, R.; Zi, J. Green production of silybin and isosilybin by merging metabolic engineering approaches and enzymatic catalysis. *Metab. Eng.* **2020**, *59*, 44−52.
(29) Andrea, M.; Comino, C.; Lanteri, S.; de Vos, R.; de Waard, P.; van Beek, T. A.; Goitre, L.; Retta, S. F.; Beekwilder, J. Production of novel antioxidative phenolic amides through heterologous expression of the plant's chlorogenic acid biosynthesis genes in yeast. *Metab. Eng.* **2010**, *12*, 223−232.
(30) Sonnante, G.; D'Amore, R.; Blanco, E.; Pierri, C. L.; De Palma, M.; Luo, J.; Tucci, M.; Martin, C. Novel hydroxycinnamoyl-coenzyme A quinate transferase genes from artichoke are involved in the synthesis of chlorogenic acid. *Plant Physiol.* **2010**, *153*, 1224−1238.
(31) Liu, Q.; Yu, T.; Li, X.; Chen, Y.; Campbell, K.; Nielsen, J.; Chen, Y. Rewiring carbon metabolism in yeast for high level production of aromatic chemicals. *Nat. Commun.* **2019**, *10*, No. 4976.
(32) Braus, G. H. Aromatic amino acid biosynthesis in the yeast *Saccharomyces cerevisiae* -a model system for the regulation of a eukaryotic biosynthetic pathway. *Microbiol. Rev.* **1991**, *55*, 349−370.
(33) Rodriguez, A.; Kildegaard, K. R.; Li, M.; Borodina, I.; Nielsen, J. Establishment of a yeast platform strain for production of *p*-coumaric acid through metabolic engineering of aromatic amino acid biosynthesis. *Metab. Eng.* **2015**, *31*, 181−188.
(34) Hassing, E. J.; de Groot, P. A.; Marquenie, V. R.; Pronk, J. T.; Daran, J. G. Connecting central carbon and aromatic amino acid metabolisms to improve *de novo* 2-phenylethanol production in *Saccharomyces cerevisiae*. *Metab. Eng.* **2019**, *56*, 165−180.
(35) Liu, H.; Tian, Y.; Zhou, Y.; Kan, Y.; Wu, T.; Xiao, W.; Luo, Y. Multi-modular engineering of *Saccharomyces cerevisiae* for high-titre production of tyrosol and salidroside. *Microb. Biotechnol.* **2021**, *14*, 2605−2616.

https://doi.org/10.1021/acssynbio.1c00487
ACS Synth. Biol. 2022, 11, 800−811

(36) Li, M.; Kildegaard, K. R.; Chen, Y.; Rodriguez, A.; Borodina, I.; Nielsen, J. *De novo* production of resveratrol from glucose or ethanol by engineered *Saccharomyces cerevisiae*. *Metab. Eng.* **2015**, *32*, 1−11.
(37) Li, M.; Schneider, K.; Kristensen, M.; Borodina, I.; Nielsen, J. Engineering yeast for high-level production of stilbenoid antioxidants. *Sci. Rep.* **2016**, *6*, No. 36827.
(38) Koopman, F.; Beekwilder, J.; Crimi, B.; Houwelingen, A. V.; Hall, R. D.; Bosch, D.; Maris, A. V.; Pronk, J. T.; Daran, J. M. *De novo* production of the flavonoid naringenin in engineered *Saccharomyces cerevisiae*. *Microb. Cell Fact.* **2012**, *11*, No. 155.
(39) Lyu, X.; Ng, K. R.; Lee, J. L.; Mark, R.; Chen, W. N. Enhancement of naringenin biosynthesis from tyrosine by metabolic engineering of *Saccharomyces cerevisiae*. *J. Agric. Food Chem.* **2017**, *65*, 6638−6646.
(40) Luttik, M. A.; Vuralhan, Z.; Suir, E.; Braus, G. H.; Pronk, J. T.; Daran, J. M. Alleviation of feedback inhibition in *Saccharomyces cerevisiae* aromatic amino acid biosynthesis: quantification of metabolic impact. *Metab. Eng.* **2008**, *10*, 141−153.
(41) Suástegui, M.; Guo, W. H.; Feng, X. Y.; Shao, Z. Y. Investigating strain dependency in the production of aromatic compounds in *Saccharomyces cerevisiae*. *Biotechnol. Bioeng.* **2016**, *113*, 2676−2685.
(42) Suástegui, M.; Yu, N. C.; Chowdhury, A.; Sun, W.; Cao, M.; House, E.; Maranas, C. D.; Shao, Z. Multilevel engineering of the upstream module of aromatic amino acid biosynthesis in *Saccharomyces cerevisiae* for high production of polymer and drug precursors. *Metab. Eng.* **2017**, *42*, 134−144.
(43) Shen, B.; Zhou, P.; Jiao, X.; Yao, Z.; Ye, L.; Yu, H. Fermentative production of Vitamin E tocotrienols in *Saccharomyces cerevisiae* under cold-shock-triggered temperature control. *Nat. Commun.* **2020**, *11*, No. 5155.
(44) Nocon, J.; Steiger, M.; Mairinger, T.; Hohlweg, J.; Russmayer, H.; Hann, S.; Gasser, B.; Mattanovich, D. Increasing pentose phosphate pathway flux enhances recombinant protein production in *Pichia pastoris*. *Appl. Microbiol. Biotechnol.* **2016**, *100*, 5955−5963.
(45) Outten, C. E.; Culotta, V. C. A novel NADH kinase is the mitochondrial source of NADPH in *Saccharomyces cerevisiae*. *EMBO J.* **2003**, *22*, 2015−2024.
(46) Li, Y.; Li, S.; Thodey, K.; Trenchard, I.; Cravens, A.; Smolke, C. D. Complete biosynthesis of noscapine and halogenated alkaloids in yeast. *Proc. Natl. Acad. Sci. U.S.A.* **2018**, *115*, E3922−E3931.
(47) Ma, T.; Shi, B.; Ye, Z.; Li, X.; Liu, M.; Chen, Y.; Xia, J.; Nielsen, J.; Deng, Z.; Liu, T. Lipid engineering combined with systematic metabolic engineering of *Saccharomyces cerevisiae* for high-yield production of lycopene. *Metab. Eng.* **2019**, *52*, 134−142.
(48) Jiang, H.; Wood, K. V.; Morgan, J. A. Metabolic engineering of the phenylpropanoid pathway in *Saccharomyces cerevisiae*. *Appl. Environ. Microbiol.* **2005**, *71*, 2962−2969.
(49) Liu, T.; Huang, Y.; Jiang, L.; Dong, C.; Gou, Y.; Lian, J. Efficient production of vindoline from tabersonine by metabolically engineered *Saccharomyces cerevisiae*. *Commun. Biol.* **2021**, *4*, No. 1089.
(50) Jiang, L.; Huang, L.; Cai, J.; Xu, Z.; Lian, J. Functional expression of eukaryotic cytochrome P450s in yeast. *Biotechnol. Bioeng.* **2021**, *118*, 1050−1065.
(51) Li, Y.; Mao, J.; Liu, Q.; Song, X.; Wu, Y.; Cai, M.; Xu, H.; Qiao, M. *De novo* biosynthesis of caffeic acid from glucose by engineered *Saccharomyces cerevisiae*. *ACS Synth. Biol.* **2020**, *9*, 756−765.
(52) Lian, J.; Zhao, H. Reversal of the beta-oxidation cycle in *Saccharomyces cerevisiae* for production of fuels and chemicals. *ACS Synth. Biol.* **2015**, *4*, 332−341.
(53) Mikkelsen, M. D.; Buron, L. D.; Salomonsen, B.; Olsen, C. E.; Hansen, B. G.; Mortensen, U. H.; Halkier, B. A. Microbial production of indolylglucosinolate through engineering of a multi-gene pathway in a versatile yeast expression platform. *Metab. Eng.* **2012**, *14*, 104−111.
(54) Apel, A. R.; d'Espaux, L.; Wehrs, M.; Sachs, D.; Li, R. A.; Tong, G. J.; Garber, M.; Nnadi, O.; Zhuang, W.; Hillson, N. J.; Keasling, J. D.; Mukhopadhyay, A. A Cas9-based toolkit to program gene expression in *Saccharomyces cerevisiae*. *Nucleic Acids Res.* **2017**, *45*, 496−508.
(55) Lian, J.; Bao, Z.; Hu, S.; Zhao, H. Engineered CRISPR/Cas9 system for multiplex genome engineering of polyploid industrial yeast strains. *Biotechnol. Bioeng.* **2018**, *115*, 1630−1635.
(56) Heigwer, F.; Kerr, G.; Boutros, M. E-CRISP: fast CRISPR target site identification. *Nat. Methods* **2014**, *11*, 122−123.
(57) Stovicek, V.; Borodina, I.; Forster, J. CRISPR-Cas system enables fast and simple genome editing of industrial *Saccharomyces cerevisiae* strains. *Metab. Eng. Commun.* **2015**, *2*, 13−22.
(58) Liu, X.; Cheng, J.; Zhang, G.; Ding, W.; Duan, L.; Yang, J.; Kui, L.; Cheng, X.; Ruan, J.; Fan, W.; Chen, J.; Long, G.; Zhao, Y.; Cai, J.; Wang, W.; Ma, Y.; Dong, Y.; Yang, S.; Jiang, H. Engineering yeast for the production of breviscapine by genomic analysis and synthetic biology approaches. *Nat. Commun.* **2018**, *9*, No. 448.
(59) Yao, Z.; Zhou, P.; Su, B.; Su, S.; Ye, L.; Yu, H. Enhanced isoprene production by reconstruction of metabolic balance between strengthened precursor supply and improved isoprene synthase in *Saccharomyces cerevisiae*. *ACS Synth. Biol.* **2018**, *7*, 2308−2316.

https://doi.org/10.1021/acssynbio.1c00487
ACS Synth. Biol. 2022, 11, 800−811